Thermodynamics of Phase Equilibria in Magma

Pascal Richet[1] and Giulio Ottonello[2]
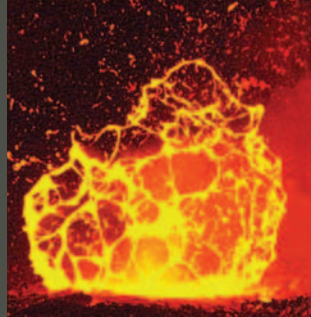
A 5 m bubble bursting during the 2004 eruption of Piton de la Fournaise (La Réunion Island), dramatically illustrating volatile release from the magma. PHOTOGRAPH: PHILIPPE MAIRINE

Throughout geological history, partial melting of mantle rocks and magma ascent and crystallization have played key roles in shaping the Earth. The importance of magmas stems from their liquid nature, that is, from their high atomic mobility and lack of long-range order. Compared to crystals, magmas thus have peculiar thermodynamic properties. A few examples illustrate how solid–liquid and liquid–volatile equilibria can be predicted. Given the almost infinite diversity of conditions of chemical composition, temperature and pressure in nature, thermodynamic modelling has become a necessary tool for understanding magmatic processes.

KEYWORDS: magma, melting, crystallization, buoyancy, configurational properties

A TOOL FOR UNDERSTANDING IGNEOUS PROCESSES

Volcanic eruptions are a most dramatic illustration of the boundless power of nature. Although magmas are the cause of these phenomena, their origin and evolution have long remained elusive. The confusion of ideas that still prevailed at the end of the 18th century is illustrated by the term *pyroxene* (from *pyros*, fire, and *xenos*, foreign), which was coined when this mineral was thought to result from incomplete melting of the source rock by subterranean fires. From clever field observations, however, Dolomieu (of dolomite fame) concluded in 1797 that lavas originated from the deep, dense, "pasty and viscous" matter upon which the solid crust rested all over the world. At the same time, experimental petrology was initiated by Hall (1798), who observed that the vitreous or stony character of the product formed when molten basalt was cooled depended on its rate of quenching. Hence, the presence of xenocrysts, such as pyroxene, in lavas was no longer seen as indicative of incomplete fusion but the result of partial crystallization of the melt.

Just as fossils were doing for sedimentary terranes, crystals came to represent a valuable source of information on igneous rocks. Accounting for the diversity of these rocks in the Earth's crust became the main goal of the fledgling discipline of igneous petrology, but it was recognized early on that a variety of tools had to be used to understand the natural record in terms of magma formation and evolution. As implicitly illustrated by the pyroxene story, thermodynamics played a critical role in this respect. Of course, experimental petrology has been of paramount importance in determining which phases are stable under given condi-

tions of temperature, pressure and chemical composition. Without the thermodynamic framework provided by the phase rule, however, interpretation of these results would be at least ambiguous, if not really thorny. Without thermodynamic modelling, interpolation or extrapolation to real processes of such experimental data, which pertain to necessarily restricted ranges of relevant conditions, would, in addition, be impossible. And this need for modelling has become even more pressing ever since the field of igneous petrology was enlarged to include Earth's mantle, which mostly escapes direct observation. In short, thermodynamics as applied to magmatic processes has now grown to such an extent that we can only highlight a few points here.

MAGMAS AS MOLTEN SUBSTANCES

Magmas owe their importance to the efficient way they transport energy and matter, at all scales, in response to pressure and temperature gradients. This efficiency results from the high atomic mobility that is the hallmark of melts, as evidenced in daily life by the easy way in which a liquid flows. Contrary to solids, either crystalline or vitreous, where atoms occupy essentially fixed positions, liquids are characterized by dynamic disorder, that is, by unceasing structural rearrangements made possible by the excess thermal energy, with respect to solids, that they acquire on melting. The nature of these structural changes is constrained by Le Châtelier's laws:

$$(\partial G/\partial T)_P = -S \quad \text{and} \quad (\partial G/\partial P)_T = V . \qquad (1)$$

Under equilibrium conditions, increases in temperature (T) and pressure (P) thus cause increases in entropy (S) and decreases in volume (V), respectively, to ensure a minimum value for the Gibbs free energy (G) of the melt. Because it scales as viscosity, the rate of these structural rearrangements decreases on cooling. If crystallization is bypassed, this rate eventually vanishes in a narrow temperature interval, the glass transition range, where the frozen-in atomic configuration of the liquid becomes the structure of a disordered solid, a glass.

From a geological standpoint, two important consequences follow. First, the disordered nature of glasses and melts allows a wide range of elements to coexist in a single phase, as illustrated by the fact that a single liquid forms through melting of a rock made up of a number of mineral phases. Second, part of the heat given to a melt does not result in a temperature increase, but in exploration of atomic positions of higher potential energy which are associated with

1 Institut de Physique du Globe de Paris, Bureau 401
   1 rue Jussieu, 75005 Paris, France
   E-mail: richet@ipgp.fr

2 Dipteris, Università di Genova, Corso Europa 26
   16132 Genova, Italia
   E-mail: giotto@dipteris.unige.it
   Send queries on calculations and data sources to G. Ottonello.

higher entropy. The heat capacity (C_p), enthalpy (H) and entropy can thus be split into two different contributions: a vibrational part, akin to the properties of solids, and a configurational part, which determines thermochemical differences between melts and crystals (FIG. 1) (Richet and Neuville 1992). A similar distinction holds for volume properties. Since the positions of higher potential energy explored by atoms in liquids are generally associated with longer interatomic distances, the density (ρ) of a melt is lower than that of a crystalline assemblage of the same composition, whereas its thermal expansion coefficient, α, given by $1/V\,(\partial V/\partial T)_P$, is higher.

For a mineral that melts without composition change, the higher entropy and lower density of the liquid compared to the crystal cause the melting temperature to increase with pressure, as stated by the Clausius-Clapeyron equation:

$$dT/dP = \Delta V_f/\Delta S_f \,, \qquad (2)$$

where ΔV_f and ΔS_f are the volume and entropy of melting. Although Equation (2) has no counterpart for calculating the variations with pressure of the liquidus and solidus temperatures of a rock, the same effect obtains because mixing in the liquid state of the individual mineral components results in further increases of the entropy of the melt. Since melting begins to take place when the geothermal gradient intersects the solidus of mantle rocks, the former curve has a steeper slope than the latter.

Importantly, the lack of long-range order in a liquid makes possible a wide range of densification mechanisms, such as pressure-induced changes of Si and Al from 4 to higher coordination by oxygen (FIG. 2); such changes are not available to a given crystal where only changes in bond angles and distances are possible if long-range symmetry is to be maintained. Because of this configurational contribution, a melt has a higher compressibility [$\beta_T = -1/V\,(\partial V/\partial P)_T$] and lower bulk modulus ($K_T = 1/\beta_T$) than its isochemical crystalline assemblage. For diopside ($CaMgSi_2O_6$), which can be used as a model system for basalt, the room-pressure bulk modulus, K_{T0}, is about 23 and 91 GPa at 1700 K for the melt and crystal, respectively (see Richet and Neuville 1992). The density contrast between these two kinds of phases (melt and crystal) thus decreases with increasing pressure, but less strongly than indicated by these figures. As illustrated by the analysis made for SiO_2 (FIG. 2), the reason is that the rate of structural rearrangements decreases with increasing pressure so that the increase of K_T with pressure is also much higher for the melt than for
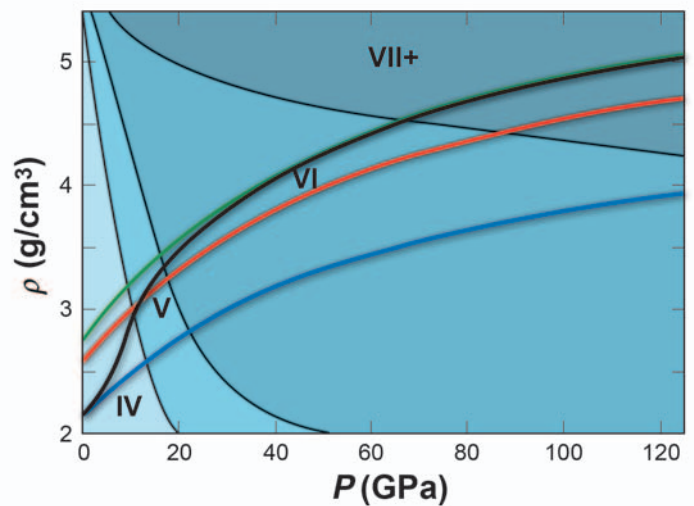

FIGURE 2 Influence of coordination changes on the high-pressure density of amorphous SiO_2 at 1200 K. The black curve represents the compression of SiO_2 as calculated by Ghiorso (2004) from the relative abundances of the various coordination states (blue areas) and the compression of each of these states (blue curve: $^{IV}SiO_2$; red: $^{V}SiO_2$; green: $^{VI}SiO_2$).

the crystal, with values of $K_{T0}' = (\partial K/\partial P)_T$ at room pressure of about 10 and 4, respectively. These parameters control both the pressure dependence of the Gibbs free energy and the buoyancy of magma, which allows it to rise from its site of formation at depth to the surface. In view of this dual importance, efforts are being made to use atomistic simulations to complement the limited database resulting from the considerable difficulty of making volume measurements on melts at very high pressures (Ghiorso 2004).

PHASE EQUILIBRIA AND THERMODYNAMIC MODELLING

As extensively determined since the first half of the 20th century, liquidus and solidus data still constitute the main source of thermodynamic information for silicate melts (see Levin et al. 1964). These data refer to conditions of chemical equilibrium, which are actually relevant to natural processes in view of their high temperatures and long timescales. The state of equilibrium that is reached eventually gets frozen in at some stage, however, when the kinetics of the reaction of interest become too slow compared with the cooling rate of the system.

An example of fundamental petrological importance for basalt and andesite petrogenesis is the melting relations of plagioclase feldspars (FIG. 3). On cooling, a melt of composition Y forms a first crystal of composition X. Depending on whether the crystal is removed from the system (fractional crystallization) or keeps equilibrating with the melt (batch crystallization), its composition varies from X to Y or from X to pure albite along the solidus, and that of the melt along the liquidus from Y to Z or from Y to pure albite, respectively. Similar differences apply for fractional and batch melting, with the consequence that the melt becomes enriched in the least refractory component whenever the transformation is not total. Analogous evolutions are observed in phase diagrams with different topologies. As expounded long ago by Bowen (1928), they are the basis of magma differentiation, which leads from basaltic to felsic melts.
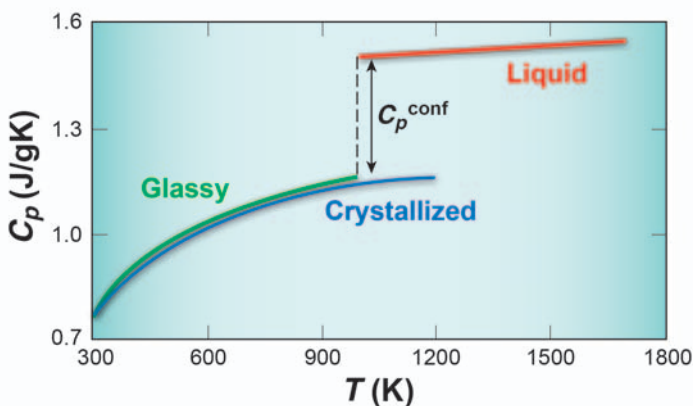

FIGURE 1 Importance of the configurational heat capacity (C_p^{conf}) of silicate melts as exemplified by the C_p differences between a fully crystallized alkali basalt and its glass and liquid phases. DATA FROM BOUHIFD ET AL. (2007)

In the simplest thermodynamic model of plagioclase melting, the end-member compositions $CaAl_2Si_2O_8$ (An, anorthite) and $NaAlSi_3O_8$ (Ab, albite) are chosen as components and are assumed to mix ideally, that is, randomly and without any thermal effect. From reported heat capacities for the liquid and solid phases and enthalpies of fusion (see Richet and Bottinga 1986), one readily calculates liquidus and solidus branches by finding the crystal (c) and liquid (l) compositions for which the chemical potential (μ) equations

$$\mu_{An}^c = \mu_{An}^l \quad \text{and} \quad \mu_{Ab}^c = \mu_{Ab}^l \qquad (3)$$

are satisfied at a given temperature (see Richet et al. 2010 this issue). Agreement with the experimental data is excellent for the liquidus and fair for the solidus (FIG. 3). As expected, ideal mixing is more clearly followed in the liquid than in the solid phase, for which better agreement is achieved through inclusion of an enthalpy term and adjustment of the entropy term to account for the lack of Al–O–Al linkages in plagioclases.

When metal oxides are added to pure SiO_2, however, the structure changes markedly from a three-dimensional open network of SiO_4 tetrahedra to the isolated SiO_4 tetrahedra of orthosilicates. This depolymerization is described by reactions such as

$$-Si-O-Si- + Na_2O <=> 2\ Si-O-Na\ , \qquad (4)$$
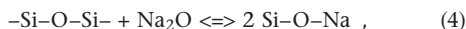
but an important difficulty of thermodynamic modelling is that there is no way to define a unique set of components relevant throughout the wide composition ranges of interest, that is, a set of components whose entropy of mixing remains close to ideal from pure-SiO_2 to SiO_2-poor melts. As a result, the numerous models found in the literature differ from one another not only by the functional forms they posit for the activity–composition relationships but also by their choices of components. In spite of their differences, most models share the common point that they can be considered as tools for performing mathematical fits whose extrapolation to composition ranges not dealt with in their calibration is problematic.

The model developed by Ghiorso and co-workers in the freeware code MELTS (http://melts.ofm-research.org) is the most extensively used in geology because it has been specifically tailored to basalt petrogenesis (Ghiorso and Sack 1995). It relies on a set of 14 components, which are either oxides (SiO_2, TiO_2, Al_2O_3, Fe_2O_3, Cr_2O_3, P_2O_5, SrO, H_2O) or more complex entities (Na_2SiO_3, K_2SiO_3, Mg_2SiO_4, Ca_2SiO_4, Mn_2SiO_4, Fe_2TiO_4), and all (except H_2O) are referred to 8 oxygen atoms (Si_4O_8, etc.). These components were selected because their thermodynamic properties could be retrieved from a combination of thermochemical and phase equilibria data and, as illustrated by modelling of plagioclase melting, because part of the complicated interactions between individual atoms is automatically taken care of when complex components are used. The Gibbs free energy of the melt is assumed to be of the so-called regular form:

$$G(P,T) = \sum n_i\ \mu_i^\circ + RT\ (\sum n_i)\ \sum x_i \ln x_i +$$
$$\frac{1}{2}\ (\sum n_i)\ \sum\sum W_{ij}\ x_i\ x_j\ , \qquad (5)$$

where n_i is the number of moles of the ith component and x_i is its mol fraction. The first term is the weighted sum of the standard state chemical potentials (μ_i°) of the components at the P–T of interest; the second is the ideal entropy of mixing; and the third is the enthalpy of mixing expressed in terms of binary interaction parameters, W_{ij}, between components i and j which are determined from fits made with Equation (5) to input phase equilibria data for complex systems only. Likewise, use is made of the non-ideal solution models available for the solid solutions
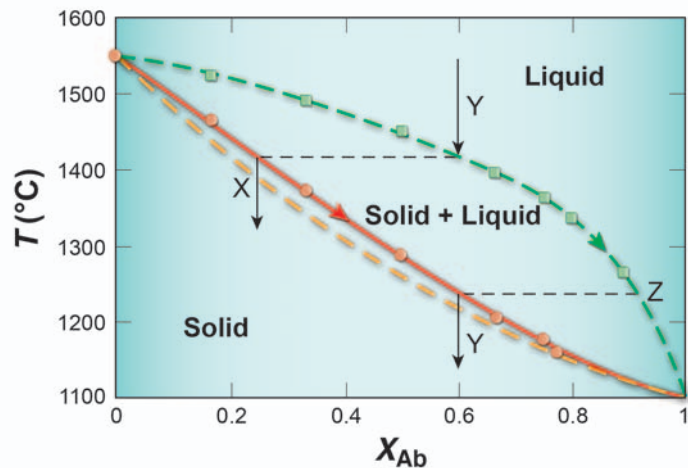
Plagioclase melting relations. The figure shows experimental data (circles and squares) (Bowen 1913) and a phase diagram calculated assuming ideal mixing of the two end-member components, albite and anorthite, in both melt and solid phases (dashed curves) or with a non-ideal model for plagioclases (solid curve). The liquidus and solidus branches are said to be univariant because, once pressure is fixed, equilibrium between the liquid and crystal is reached at a single temperature for a given composition or, conversely, for a single composition at a given temperature. X_{Ab} is the molar proportion of albite in the system albite–anorthite. The compositions X, Y and Z are discussed in the text.

of interest, such as spinels, olivines, pyroxenes and plagioclases. For given pressure, temperature and composition, equilibrium is reached when G is minimum, whereas the nature and composition of the solid phases is such that chemical potential equalities analogous to Equation (3) are satisfied for all components. The predictions of energy and chemical evolution as a function of pressure, temperature, oxygen fugacity and water content made reliably with this model are now well established. As for the effects of pressure, Ghiorso and co-workers are working to extend equations of state to 100 GPa and 5000 K with the help of atomistic simulations.

Alternatively, only oxide components have been used by Pelton and co-workers to set up the "quasi-chemical" model at the core of the FACT commercial package (e.g. Pelton and Wu 1999). This model is probably the most popular in metallurgy and the glass industry because it depicts the topological complexity of phase diagrams with unmatched precision thanks to the long series expansion used for both enthalpy and entropy contributions to the activity. For instance, 6, 4 and 4 fit parameters are introduced for the binary systems CaO–SiO_2, CaO–Al_2O_3 and Al_2O_3–SiO_2, respectively, whereas 2 ternary interaction parameters are in addition needed for CaO–Al_2O_3–SiO_2 melts (Eriksson and Pelton 1993). The results obtained for this complex phase diagram of enormous industrial interest illustrate the usefulness of the method. The effects of pressure, however, are not accounted for.

VOLATILE DISSOLUTION

Undoubtedly, the most spectacular illustration of the role played by volatiles in melts is the kilometre-high column of a Plinian eruption, where millions of tons of ejecta are self-sustained by a jet of gases exsolved at the fragmentation level with a velocity of several hundred metres per second. Understanding the way in which volatile solubility depends on pressure, temperature and composition is thus an important issue. The assumption that volatiles dissolve in a melt in molecular form can be made for only a few

species, such as the noble gases, He, Ne, Ar, Kr and Xe (Lux 1987). In contrast, the major volatiles H_2O, CO_2 and SO_2 have a complex reactive solubility. This is why water induces large melting point depressions, which reach for instance 800 K for quartz at a pressure of 1 GPa (FIG. 4).

Comprehensive models have been set up for dealing with H_2O and CO_2 dissolution (e.g. Papale et al. 2006). For illustration purposes, however, a simple regular-type solution model analogous to Equation (5) broadly accounts for the trend of FIGURE 4. Written in terms of the chemical potential, equilibrium between quartz and SiO_2 in the melt implies that

$$\mu_{SiO_2}{}^c = \mu_{SiO_2}{}^l = \mu^°_{SiO_2}{}^l + RT \, [\ln (1 - x_{H_2O}) + W_{Si-H} \, x_{H_2O}{}^l] \, , \qquad (6)$$

where $\mu^°_{SiO_2}{}^l$ is the chemical potential of pure SiO_2 melt at the T–P of interest, $x_{H_2O}{}^l$ is the water mol fraction in the liquid and W_{Si-H} is an interaction parameter. Under dry conditions, the increase of the melting temperature of quartz with pressure is calculated without any fit parameter from available volume and thermochemical data for quartz and SiO_2 melt (FIG. 4). Under wet conditions, a pressure-dependent interaction parameter, W_{Si-H} (kJ) = –22.4 + 1.94 P (kbar), is needed in Equation (6) to match the experimental liquidus and water solubility data along the liquidus (FIGS. 4, 5). This negative term enhances slightly the large decrease of $\mu_{SiO_2}{}^l$ originating in the entropy of mixing term of Equation (6), which causes the strong decrease of the melting temperature under water pressure. As for the water solubilities calculated in this way, they do not vary linearly with the square root of water fugacity (see below) and become too low at the highest pressures (FIG. 5). Excellent agreement with the experimental data requires a more complicated model with either more fit parameters or at least two water species instead of the single one embodied in Equation (6). This illustrates the usual trade-off that can be made between the choice of components of structural significance and the use of activity–composition relationships with a high number of fit parameters.

The complex reactive solubility of H_2O, CO_2 and SO_2 is in fact intimately related to the acid–base properties of these species. These features can be addressed with a third kind of thermodynamic model based on a polymeric description of silicate melts (Ottonello 2001; Ottonello et al. 2001; Moretti and Ottonello 2005). The starting point is the equilibrium between the various oxygen species in the liquid, i.e. O^0 (bridging), O^- (non-bridging) and O^{2-} (free), which lies behind Equation (4):

$$O^0 + O^{2-} <=> 2 \, O^- \, . \qquad (7)$$
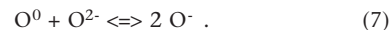
It appears that CO_2 is an acidic oxide because it accepts an electron when reacting with a free oxygen ion, O^{2-}, of the melt to form a carbonate ion:

$$CO_2 + O^{2-} <=> CO_3{}^{2-} \, . \qquad (8)$$
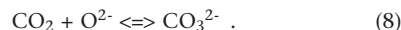
As observed (see Mysen and Richet 2005), the solubility of CO_2 is favoured in basic melts, where Equation (8) is displaced to the right-hand side. In contrast, water is a basic oxide as it depolymerizes the silicate network in the same way as metal oxides [see Equation (4)], and creates hydroxyl (OH) terminations:

$$-Si–O–Si + H_2O <=> 2 \, Si–O–H \, . \qquad (9)$$
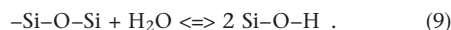
This reaction predominates in the first stage of dissolution, before dissolved molecular water must also be taken into account, as indicated by spectroscopic studies (e.g. Stolper 1982). Denoting by K the equilibrium constant of Equation (9), we write that water solubility is then proportional to the square root of the water fugacity in the gaseous phase, f_{H_2O}:

$$x_{H_2O} = 1/2 \, (K \, f_{H_2O} \, [O^0])^{1/2} \, , \qquad (10)$$

where $[O^0]$ is the mol fraction of bridging oxygens. These differing solution mechanisms of H_2O and CO_2 manifest themselves in phase equilibria. As an example, the primary phase field of forsterite in the CaO–MgO–Al_2O_3–SiO_2 system expands and contracts upon dissolution of H_2O or CO_2, respectively, whereas that of enstatite correlatively varies in the opposite way (Kushiro and Yoder 1968).

CONCLUSIONS

Although modelling complexities have not been considered, this review illustrates how solid–liquid and fluid–liquid equilibria can be calculated throughout the extremely wide P–T range relevant to magmatic activity. Of course, such predictions are most reliable at lower
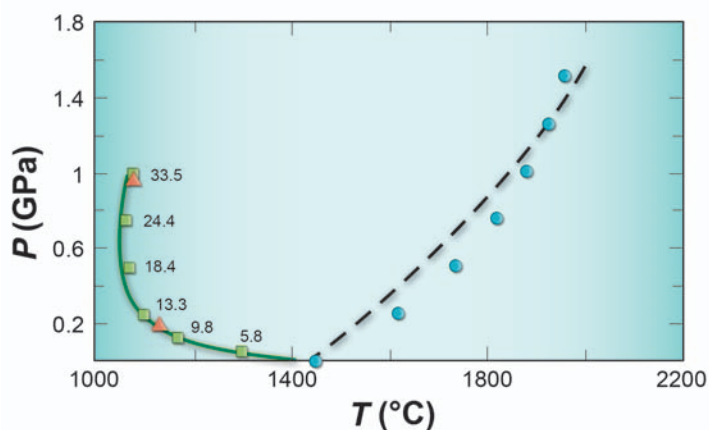
FIGURE 4 Melting curve of quartz under dry (dotted line) and wet (green line) conditions. The diagram shows experimental data (Jackson 1976; Boettcher 1984) and P–T curves calculated with Equation (6) and the relevant thermochemical and elastic data. The numbers shown are water solubilities (mol% H_2O) calculated along the wet liquidus.
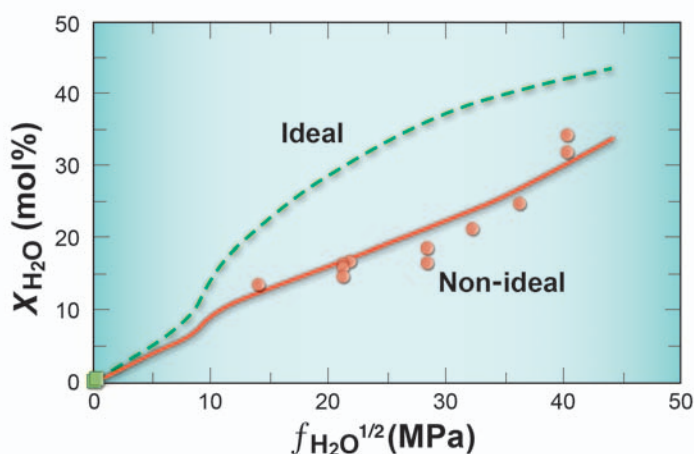
FIGURE 5 Water solubility (X_{H_2O}) in an SiO_2 melt against the square root of water fugacity (f_{H_2O}). The experimental data are from Kennedy et al. (1962) and the values have been calculated with the assumption of either an ideal solution model (dashed curve) or the non-ideal model of Equation (6) (solid curve).

pressures where models are calibrated with abundant experimental data. But high pressures are also of fundamental interest because magma forms at great depth. In subduction zone settings, melting results from reaction of solid peridotite with the water released when the oceanic lithosphere is subducted, producing magmas that eventually yield the andesite lava series (Grove et al. 2006). The basalt lava series originates via decompression of peridotite in convecting cells ascending at speeds of a few centimetres per year. Thermodynamically, the process has been described in different ways that cannot be summarized in a few lines (see Ganguly 2005; Stolper and Asimow 2007). Suffice it to say that as a first approximation, the heat exchanged by the plume with its surroundings can be neglected, so that magma ascent takes place under adiabatic conditions. Melting is then triggered by the pressure decrease, which causes the solidus curve of mantle peridotites to intersect the geothermal gradient at depths of the order of 100 km.

Two final points will be mentioned. First, the rates of magma ascent and volatile exsolution strongly depend on melt viscosity. Viscosity is closely related to atomic mobility and is quantitatively related to configurational entropy, the thermodynamic measure of disorder. Investigation of the thermodynamic properties of melts thus has clear implications for the temperature, pressure and composition dependencies of viscosity (e.g. Richet 2009). The second point deals with crystallization, which can be assumed to take place under equilibrium conditions only between the solidus and liquidus. At high degrees of supercooling, crystallization proceeds irreversibly instead, and kinetic factors need to be considered. Of particular significance is that crystals are often metastable and tend to be structurally disordered and non-stoichiometric, being enriched in the elements that diffuse fastest in the melt, that is, in network-modifier cations (Bouhifd et al. 2004; Roskosz et al. 2006); in such cases, the models presented in this review no longer apply.
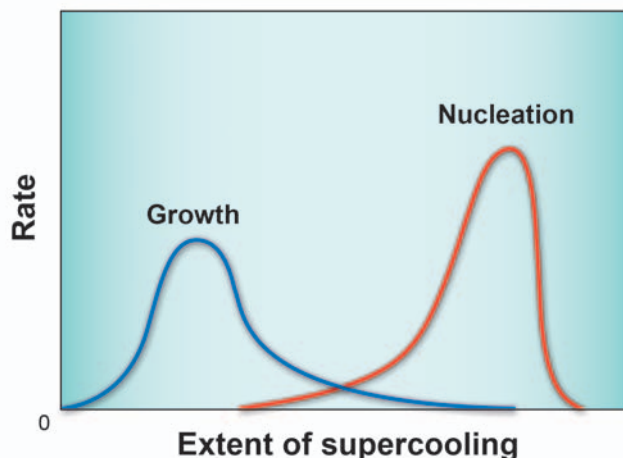
That kinetic factors are important is also shown by the differences in texture between volcanic and plutonic rocks. Crystal formation is described as a two-step process: nucleation and crystal growth, whose rates vary in different ways with the extent of supercooling (FIG. 6). Depending on the time–temperature history, two limiting cases are distinguished. In plutonic rocks, crystal growth predominates over nucleation, yielding a few, large crystals. In volcanic rocks, in contrast, the small size of crystals and the presence of a glassy or microcrystalline matrix indicate instead abundant nucleation and short-lived crystal growth. Consideration of kinetic factors is, therefore, a necessary complement to equilibrium thermodynamics when attempting to reconstruct the history of a magmatic system. ∎

REFERENCES

Boettcher AL (1984) The system SiO_2–H_2O–CO_2: melting, solubility mechanisms of carbon, and liquid structure to high pressures. American Mineralogist 69: 823-833

Bouhifd MA, Richet P, Besson P, Roskosz M, Ingrin J (2004) Redox state, microstructure and viscosity of a partially crystallized basalt melt. Earth and Planetary Science Letters 218: 31-44

Bouhifd MA, Besson P, Courtial P, Gérardin C, Navrotsky A, Richet P (2007) Thermochemistry and melting properties of basalt. Contributions to Mineralogy and Petrology 153: 689-698

Bowen NL (1913) The melting phenomena of plagioclase feldspars. American Journal of Science 35: 577-599

Bowen NL (1928) The Evolution of the Igneous Rocks. Princeton University Press, Princeton

Dolomieu D de (1797) Rapport fait par le citoyen Dolomieu, Ingénieur des Mines, sur ses voyages de l'an V et de l'an VI. Journal des Mines 7: 385-402

Eriksson G, Pelton AD (1993) Critical evaluation and optimization of the thermodynamic properties and phase diagrams of the CaO-Al_2O_3, Al_2O_3-SiO_2, and CaO-Al_2O_3-SiO_2 systems.

Metallurgical and Materials Transactions B24: 807-816

Ganguly J (2005) Adiabatic decompression and melting of mantle rocks: An irreversible thermodynamic analysis. Geophysical Research Letters 32: LO6312, doi:10.1029/2005GL022363

Ghiorso MS (2004) An equation of state for silicate melts. I. Formulation of a general model. American Journal of Science 304: 637-678

Ghiorso MS, Sack RO (1995) Chemical mass transfer in magmatic processes IV. A revised and internally consistent thermodynamic model for the interpolation and extrapolation of liquid-solid equilibria in magmatic systems at elevated temperatures and pressures. Contributions to Mineralogy and Petrology 119: 197-212

Grove TL, Chatterjee N, Parman SW, Médard E (2006) The influence of H_2O on mantle wedge melting. Earth and Planetary Science Letters 249: 74-89

Hall J (1798) Curious circumstances upon which the vitreous or the stony character of whinstone and lavas respectively depend; with other facts. Journal of Natural Philosophy, Chemistry and the Arts 2: 285-288

Jackson I (1976) Melting of the silica isotypes SiO_2, BeF_2 and GeO_2 at elevated pressures. Physics of the Earth and Planetary Interiors 13: 218-231

Kennedy GC, Wasserburg GJ, Heard HC, Newton RC (1962) The upper three-phase region in the system SiO_2–H_2O. American Journal of Science 260: 501-521

Kushiro I, Yoder HS Jr (1968) Melting of forsterite and enstatite at high pressures under hydrous conditions. Carnegie Institution of Washington Yearbook 67: 153-158

Levin EM, Robbins CR, McMurdie HF (1964) Phase Diagrams for Ceramists, Second Edition. American Ceramics Society, Columbus, Ohio, 601 pp

Lux G (1987) The behavior of noble gases in silicate liquids: Solution, diffusion, bubbles and surface effects, with applications to natural samples. Geochimica et Cosmochimica Acta 51: 1549-1560

Moretti R, Ottonello G (2005) Solubility and speciation of sulfur in silicate melts: The Conjugated Toop-Samis-Flood-Grjotheim (CTSFG) model. Geochimica et Cosmochimica Acta 69: 801-823

Mysen BO, Richet P (2005) Silicate Glasses and Melts: Properties and Structure. Elsevier, Amsterdam

Ottonello G (2001) Thermodynamic constraints arising from the polymeric approach to silicate slags: the system CaO–FeO–SiO$_2$ as an example. Journal of Non-Crystalline Solids 282: 72-85

Ottonello G, Moretti R, Marini L, Vetuschi Zuccolini M (2001) Oxidation state of iron in silicate glasses and melts: a thermochemical model. Chemical Geology 174: 157-179

Papale P, Moretti R, Barbato D (2006) The compositional dependence of the saturation surface of H$_2$O + CO$_2$ fluids in silicate melts. Chemical Geology 229: 78-95

Pelton AD, Wu P (1999) Thermodynamic modeling in glass-forming melts. Journal of Non-Crystalline Solids 253: 178-191

Richet P (2009) Residual and configurational entropy: Quantitative checks through applications of Adam–Gibbs theory to the viscosity of silicate melts. Journal of Non-Crystalline Solids 355: 628-635

Richet P, Bottinga Y (1986) Thermochemical properties of silicate glasses and melts: A review. Reviews of Geophysics 24: 1-25

Richet P, Neuville DR (1992) Thermodynamics of silicate melts: Configurational properties. In: Saxena SK (ed) Advances in Physical Geochemistry 10, pp 132-161

Richet P, Henderson GS, Neuville DR (2010) Thermodynamics: The oldest branch of Earth sciences? Elements 6: 287-292

Roskosz M, Toplis MJ, Richet P (2006) Kinetic vs. thermodynamic control of crystal nucleation and growth in molten silicates. Journal of Non-Crystalline Solids 352: 180-184

Stolper E (1982) Water in silicate glasses: An infrared spectroscopic study. Contributions to Mineralogy and Petrology 81: 1-17

Stolper E, Asimow P (2007) Insights into mantle melting from graphical analysis of one-component systems. American Journal of Science 307: 1051-1139 ∎